

# Nanostructure fabrication via direct writing with atoms focused in laser fields

R. E. Scholten, J. J. McClelland, E. C. Palm, A. Gavrin, and R. J. Celotta<sup>a)</sup>

*Electron Physics Group, National Institute of Standards and Technology, Gaithersburg, Maryland 20899*

(Received 9 August 1993; accepted 3 February 1994)

The techniques of atom optics can be applied during the deposition of atoms onto a surface to produce nanostructures. A laser is used to form a standing wave intensity pattern in front of the substrate. An atom beam, which has been collimated by optical means, is focused onto the substrate by dipole forces from the standing wave pattern so as to deposit a series of lines spaced by half the laser wavelength. We describe the fabrication of a Cr nanograting formed using this new technique. The experimental arrangement for deposition and the optical collimation of the atom beam are described. Scanning electron microscopy (SEM) and atomic force microscopy (AFM) images of the resulting nanostructures are presented.

## INTRODUCTION

The technology for fabricating microscopic structures, in particular semiconductor devices, has advanced significantly since the first integrated circuits. There has been a continual trend towards ever smaller features, fueled by demands for increased speed and reduced cost, but future progress must eventually be limited by physical constraints. For example, using optical lithography, diffraction limits the dimensions of the smallest features to roughly the wavelength of the light used.

The experiments described in this paper explore a new process for simultaneously fabricating large numbers of nanometer-size structures. A beam of neutral atoms is focused using the optical forces of near-resonant laser light. The laser light acts as an array of microscopic "atom lenses," focusing the atoms in a pattern defined by variations in the laser intensity, as they deposit onto a substrate.

## ATOM OPTICS

Recent advances in the field of atom optics have demonstrated several techniques for manipulating neutral atom beams. For example, microfabricated gratings and Fresnel lenses have been used for interferometry and to image and focus an atomic beam.<sup>1</sup> However, the dimensions of the microgratings and Fresnel zone plates scale with the de Broglie wavelength  $\lambda_{dB}$  of the atoms. In order to obtain the short focal lengths desirable for nanolithography, it becomes extremely difficult to make practical nanoscopic atom optical elements.

With the development of tunable narrow bandwidth lasers, the interactions between light and atoms have become the basis for significant new developments in atom optics. In particular, the manipulation and control of atoms with lasers, which began with the idea of atom cooling,<sup>2</sup> has led to the prospect of focusing atomic beams to subwavelength dimensions for the fabrication of microscopic structures.

Light interactions with atoms can be divided into two forces: the spontaneous force and the dipole force. The spontaneous force arises from the near-resonant absorption by an

atom of a photon from the laser, followed by (on average) isotropic spontaneous emission. There is a net momentum transfer of one photon momentum to the atom in the direction of propagation of the laser beam. This process repeats at a rate limited by the spontaneous decay rate (depending on laser intensity) and hence the atom can be accelerated quite rapidly, e.g., on the order of  $10^5$  m/s<sup>2</sup> for chromium atoms.

The dipole force, also known as the gradient force, is due to the interaction between the electric field of the light and the induced electric dipole of the atom. The atoms feel a force proportional to the intensity gradient, towards either high or low intensity regions, depending on whether the laser frequency is below (red detuning) or above (blue detuning) the natural atomic resonance frequency, respectively. Both forces depend on the strength of the atomic transition, on the intensity of the laser field, and on the laser detuning with respect to the atomic resonance frequency.

The first experiments in atom focusing by Bjorkholm *et al.*<sup>3</sup> used an atomic beam propagating coaxially with a Gaussian laser beam. Red detuning was used so that the dipole force attracted atoms to the peak intensity at the center of the laser beam. Spot sizes were limited to about 28  $\mu$ m due to the perturbing effects of the relatively large spontaneous forces in the high intensity core. Balykin and Letokhov<sup>4</sup> suggested an improved configuration, using an atomic lens formed by focusing a TEM<sub>01</sub><sup>\*</sup> mode laser, again with a coaxial collimated atomic beam. The TEM<sub>01</sub><sup>\*</sup> mode is rotationally symmetric about the propagation axis, but has a zero-field core. By detuning the laser to the blue, the dipole force would attract atoms to the low field at the core, where spontaneous forces would be minimized. McClelland and Scheinfein<sup>5</sup> used a semiclassical approach to predict spot sizes down to 1 nm for this atomic lens under realistic conditions. Although this coaxial laser/atom beam configuration promises very tight focusing, its application to nanoscale device fabrication is limited since atomic focusing, and therefore deposition, is controlled only over a very small area at the center of the laser. This implies a serial patterning technique similar to that of conventional electron beam lithography.

Atomic lenses using the dipole force can be formed by any gradient in light intensity. Optical interference patterns

<sup>a)</sup>e-mail: celotta@epg.nist.gov.

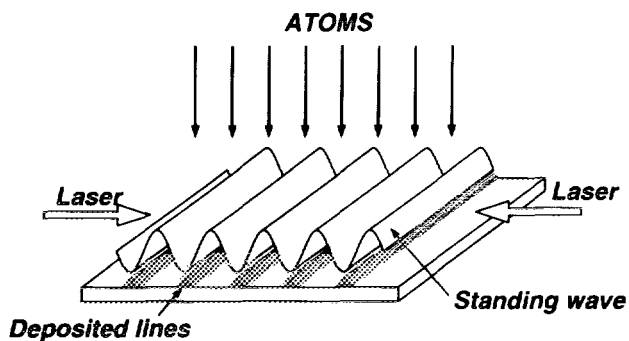


FIG. 1. A standing wave laser field forms a series of cylindrical lenses for chromium atoms, focusing them into nanometer-sized lines as they deposit onto a substrate.

provide intensity gradients which have dimensions that are inherently small, since they are directly related to optical wavelengths. A standing wave, the simplest of interference patterns, formed the basis of a more practical atomic lens used by Sleator *et al.*<sup>6</sup> to focus metastable He atoms. A cylindrical lens potential was created by a single period of the standing wave (SW) perpendicular to the atomic beam. The SW was formed above a mirror by reflection at a near-grazing incidence angle (12 mrad) to provide an unusually large period of 45  $\mu\text{m}$ . A single SW period was used to focus atoms down to a spot size of 4  $\mu\text{m}$ , and also to image a grating which had a period of 8  $\mu\text{m}$ . Timp *et al.*<sup>7</sup> used multiple periods of a standing wave as an array of cylindrical lenses, focusing a collimated sodium beam into parallel lines during deposition onto a substrate. The parallel lines, each narrower than the SW period of 295 nm, produced a periodic structure which was detected using conventional optical diffraction.

Our experiments<sup>8</sup> have used a SW to focus chromium atoms while depositing onto a silicon substrate, with a technique similar to that used by Timp *et al.* to focus sodium atoms. Chromium has several advantages; in particular it is relatively robust in air, allowing analysis of the deposited structures by various means, especially scanning electron microscopy (SEM) and atomic force microscopy (AFM), even after removal from vacuum. Chromium has an optical transition from the ( ${}^7S_3$ ) ground state to the ( ${}^7P_4^0$ ) excited state at wavelength  $\lambda=425.55$  nm (in vacuum). This transition, which has a natural linewidth of  $\Gamma=5$  MHz, is accessible with a single frequency dye laser operating with stilbene 420 laser dye. Naturally occurring Cr is 84%  $\text{Cr}^{52}$ , which has no complicating hyperfine structure. Chromium may also have direct application, e.g., as a mask for reactive ion etching or optical lithography.

## METHOD

Figure 1 illustrates the standing wave atom focusing arrangement. The SW is formed by interference between an incident laser beam, which grazes the substrate surface, and the retroreflecting beam from a mirror fixed at  $90^\circ$  to the substrate. The SW frequency is usually tuned above resonance so that the atoms are attracted to the SW nodes, where

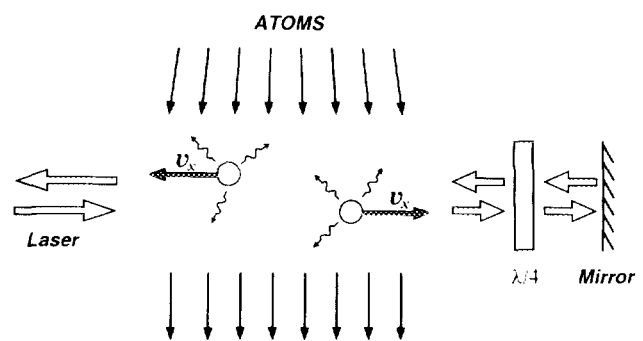


FIG. 2. Transverse laser cooling. The linearly polarized laser beam is incident from the left with a frequency below the atomic resonance. Atoms with a velocity component  $v_x$  towards the incident laser (left) will be Doppler shifted closer to resonance, and therefore more likely to absorb photons. These atoms reradiate isotropically (on average), therefore gaining momentum from the laser, resulting in a reduced transverse velocity. Similarly, atoms with a velocity component towards the reflected laser (right) will gain momentum from the right. The quarter-wave retarder ( $\lambda/4$ ) and mirror produce a reflected beam with linear polarization perpendicular to the incident beam to produce polarization gradients for sub-Doppler cooling.

the field intensity is minimum, to reduce the diffusive effects of spontaneous forces. The intensity variations within the SW create a series of parallel potential wells, spaced  $\lambda/2$  (213 nm) apart, aligned perpendicular to the atomic beam. These potential wells act as an array of microscopic cylindrical lenses, focusing the atoms into parallel lines as they deposit onto the substrate.

The atom beam must be highly collimated before focusing in the SW, because the depth of the dipole potential wells is very small compared to the transverse thermal kinetic energy of the atoms. Only those atoms with a transverse kinetic energy smaller than the dipole potential depth will be focused, while those with greater energies will skip across the wells. For typical conditions, using a 20 mW incident laser beam with a diameter of 0.4 mm tuned 40  $\Gamma$  (200 MHz) above the Cr resonance, the potential depth is approximately 0.5  $\mu\text{eV}$ , corresponding to a transverse velocity of about 1.4 m/s. To ensure that a large fraction of the thermal atoms have sufficiently small transverse velocities, the collimation angle must be approximately 1 mrad or less.

This degree of collimation could conceivably be obtained using simple collimating apertures. However, Balykin *et al.*<sup>9</sup> have shown that the spontaneous force can be used to cool an atom beam in the transverse direction. Two counterpropagating laser beams, tuned slightly below the atomic resonance frequency, intersect the atom beam at right angles (Fig. 2). Atoms which have a velocity component transverse to the atomic beam, and therefore towards one of the counterpropagating laser beams, will see laser light Doppler shifted closer to resonance. They will be more likely to absorb momentum from the laser than those atoms with smaller transverse velocities. This momentum is dissipated through spontaneous emission, until the transverse velocity is reduced to the Doppler limit, where laser heating and cooling effects balance. This scheme is enhanced by a second cooling mechanism, which relies on the magnetic sublevel structure of Cr, and on polarization gradients resulting from orthogonal linear polar-

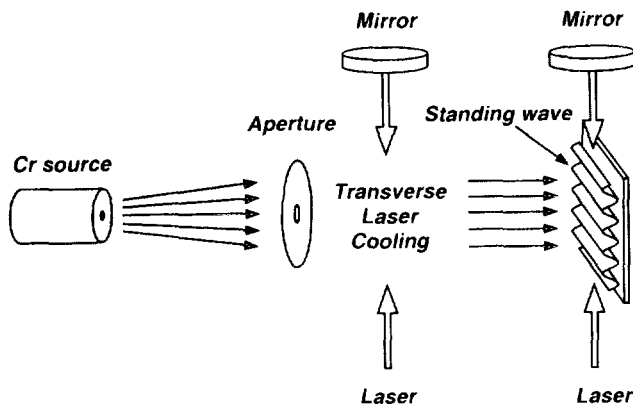


FIG. 3. Schematic of the experiment, showing Cr source, collimating aperture, transverse laser cooling, standing wave, and substrate. The atoms are collimated in the transverse laser cooling region before they are focused by the standing wave. The dye laser frequency is set above the atomic resonance by 60 to 240 MHz. The laser cooling beams are frequency shifted with an acousto-optic modulator to just below the atomic resonance.

ization in the counterpropagating laser beams.<sup>10</sup> Residual divergence angles of less than 0.2 mrad were measured. To obtain equivalent collimation without laser cooling, e.g., using two 1 mm apertures separated by 5 m, would result in a flux loss of greater than 90%.

Figure 3 shows the arrangement of effusive cell, collimating aperture, transverse laser cooling, standing wave and deposition substrate. The atomic beam is produced with a radiatively heated effusive cell at 1575 °C, and precollimated to 6 mrad with an aperture before the region of transverse laser cooling described above. The cooling laser beam is derived from the standing wave beam with a partially reflecting beam splitter, and frequency shifted with an acousto-optic modulator.

The standing wave was nominally Gaussian in profile, circularly polarized, and focused such that its waist was located at the mirror surface. The substrate position was adjusted to occlude half the standing wave so that the standing wave intensity was maximum at the surface, with a half-Gaussian intensity profile.

## RESULTS

The chromium was deposited on silicon [111] wafers with a native oxide surface. After deposition, the samples were examined by SEM and AFM. Well-defined lines with regular spacing and profile were observed over the full area covered by the standing wave and atomic beams.

A representative SEM image is shown in Fig. 4. The area depicted is approximately  $4 \times 5 \mu\text{m}$ . The sample was fabricated with an incident laser power of  $20 \pm 2 \text{ mW}$ ,<sup>11</sup> a blue detuning of  $198 \pm 2 \text{ MHz}$  and an approximately Gaussian profile with  $1/e^2$  width of  $0.39 \pm 0.02 \text{ mm}$  perpendicular to the substrate, and  $0.47 \pm 0.02 \text{ mm}$  parallel to the surface. The deposition rate was  $0.7 \pm 0.2 \text{ nm per minute}$  as determined using a quartz crystal microbalance, and the sample was exposed for a total of 10 min, giving an average chromium thickness of  $7 \pm 2 \text{ nm}$ .

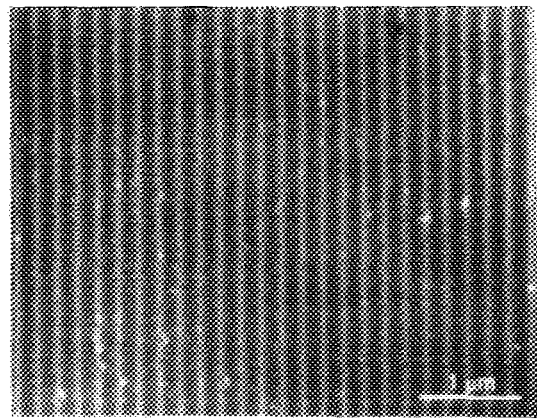


FIG. 4. Scanning electron micrograph of chromium lines on silicon created by laser focused atomic deposition. The image shows a  $4 \times 5 \mu\text{m}$  subregion of the  $0.4 \times 1 \text{ mm}$  area covered by the lines. The image was taken using a high-resolution field emission microscope, with a beam spot size of approximately 10 nm.

In Fig. 5 an AFM image shows the surface topography of a sample deposited using similar experimental parameters. The scan covers an area of approximately  $8 \times 8 \mu\text{m}$ . The peak height depends on the atomic flux and the deposition time, and on the position within the standing wave laser beam. The area shown has peaks of height  $8 \pm 2 \text{ nm}$ , where the uncertainty is due to symmetric uncertainty in the AFM calibration. Line heights of 34 nm have been demonstrated,<sup>8</sup> and recent depositions show line thicknesses in excess of 100 nm, as observed with high-resolution SEM.

Note that there is a background layer of chromium which is not apparent in this topographic image. This background is the result of unfocused chromium atoms, e.g., from other isotopes which have different transition frequencies, and atoms which were insufficiently collimated by the transverse laser cooling, particularly at the edges of the SW where the dipole potential depth is minimal. Further investigation is underway using SEM imaging of sectioned samples.

Using AFM line profiles from several samples fabricated under similar conditions, the average full width at half-maximum (FWHM) of the peaks was found to be  $65 \pm 6 \text{ nm}$ . The width is not corrected for the shape of the AFM tip,

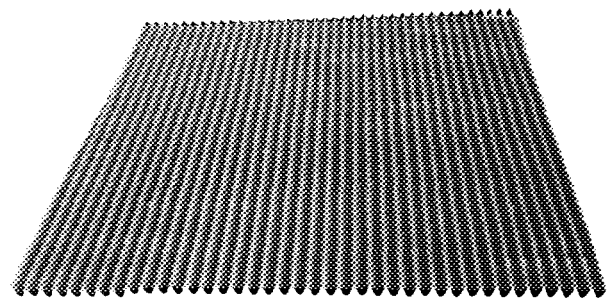


FIG. 5. Atomic force microscope image, shown in perspective, of chromium lines created by laser focused atomic deposition. The image shows an  $8 \times 8 \mu\text{m}$  subregion of the  $0.4 \times 1 \text{ mm}$  area covered by the lines. The vertical scale is expanded for illustrative purposes; the true peak height, as determined by the AFM, is  $8 \pm 2 \text{ nm}$ . The narrow ridges running horizontally, i.e., along the AFM scan direction, are image artifacts.

which is a  $70^\circ$  square pyramidal structure with a 10 to 20 nm radius point. Line profiles, and the effects of tip shape, are considered in greater detail elsewhere.<sup>8</sup>

## SUMMARY

These experiments show that atom optical techniques can be used to create, in parallel, a well-ordered array of nanometer-scale lines covering a macroscopic area. These methods might be extended to other atoms such as silver and aluminum, or to create more complex arbitrary patterns. For example, a superposition of two orthogonal standing waves will create a two-dimensional array of potential wells, so that the atoms will be focused into a similar array of spots, separated by  $\lambda/2$  in each direction. By scanning the substrate during deposition, each unit cell of the array will contain an identically painted pattern, with over two billion such patterns per square centimeter. Alternatively, a pattern of laser intensity gradients extending over a larger area, perhaps created holographically, may allow fabrication of more complex designs.

While line widths of 60 to 70 nm are narrow by comparison with current optical lithography, much smaller linewidths should be possible. Initial calculations, based on a semiclassical model, predict widths of a few nanometers given a

monochromatic atom beam with perfect collimation.<sup>8</sup> Approaching these widths will allow deposition of quite complex patterns within a single  $\lambda/2$  cell.

## ACKNOWLEDGMENTS

We would like to thank Joseph Fu for assistance in obtaining AFM images. This work was supported in part by NSF Grant No. PHY-9312572.

- <sup>1</sup>O. Carnal and J. Mlynek, *Phys. Rev. Lett.* **66**, 2689 (1991); O. Carnal, M. Sigel, T. Sleator, H. Takuma, and J. Mlynek, *ibid.* **67**, 3231 (1991).
- <sup>2</sup>T. Hänsch and A. Schawlow, *Opt. Commun.* **13**, 68 (1975); D. Wineland and H. Dehmelt, *Bull. Am. Phys. Soc.* **20**, 637 (1975).
- <sup>3</sup>J. E. Bjorkholm, R. R. Freeman, A. Ashkin, and D. B. Pearson, *Phys. Rev. Lett.* **41**, 1361 (1978); *Opt. Lett.* **5**, 111 (1980).
- <sup>4</sup>V. I. Balykin and V. S. Letokhov, *Opt. Commun.* **64**, 151 (1987).
- <sup>5</sup>J. J. McClelland and M. R. Scheinfein, *J. Opt. Soc. Am. B* **8**, 1974 (1991).
- <sup>6</sup>T. Sleator, T. Pfau, V. Balykin, and J. Mlynek, *Appl. Phys. B* **54**, 375 (1992).
- <sup>7</sup>G. Timp, R. E. Behringer, D. M. Tennant, J. E. Cunningham, M. Prentiss, and K. K. Berggren, *Phys. Rev. Lett.* **69**, 1636 (1992).
- <sup>8</sup>J. J. McClelland, R. E. Scholten, E. C. Palm, and R. J. Celotta, *Science* **262**, 877 (1993).
- <sup>9</sup>V. I. Balykin, V. S. Letokhov, and A. I. Sidorov, *JETP Lett.* **40**, 1026 (1984).
- <sup>10</sup>C. Cohen-Tannoudji and W. D. Phillips, *Physics Today* **43**, 33 (1990).
- <sup>11</sup>Error estimates quoted in this paper are to be interpreted as one standard deviation combined random and systematic errors unless otherwise indicated.